

# Depth-based Outlier Detection for Grouped Smart Meters: a Functional Data Analysis Toolbox

A. Elías, J. M. Morales, and S. Pineda,

**Abstract**—Smart metering infrastructures collect data almost continuously in the form of fine-grained long time series. These massive time series often have common daily patterns that are repeated between similar days or seasons and shared between grouped meters. Within this context, we propose a method to highlight individuals with abnormal daily dependency patterns, which we term *evolution outliers*. To this end, we approach the problem from the standpoint of Functional Data Analysis (FDA), by treating each daily record as a function or curve. We then focus on the morphological aspects of the observed curves, such as daily magnitude, daily shape, derivatives, and inter-day evolution. The proposed method for evolution outliers relies on the concept of *functional depth*, which has been a cornerstone in the literature of FDA to build shape and magnitude outlier detection methods. In conjunction with our evolution outlier proposal, these methods provide an outlier detection toolbox for smart meter data that covers a wide palette of functional outliers classes. We illustrate the outlier identification ability of this toolbox using actual smart-metering data corresponding to photovoltaic energy generation and circuit voltage records.

**Index Terms**—outlier detection, evolution outlier, smart meters, functional data analysis, functional time series, functional depth measures.

## I. INTRODUCTION

**S**MART metering infrastructures are spreading and with them the ability to improve the quality, efficiency, and sustainability of electricity systems. Nowadays, numerous features such as energy consumption, household circuit voltage, and photo-voltaic energy generation are available for long time periods, at a very high-frequency rate. Furthermore, these features are contemporaneously collected for a multitude of grouped meters. For example, residential smart meters record data from different households in a given neighborhood or city [1]. Another example is a solar energy farm collecting power generation data at the inverter level, providing as many time series as inverters [2].

Within this framework, outlier detection has become a topic of interest in the context of smart meter analysis [3]. Indeed, the technical literature reports that the results in the presence of outliers in smart meter data cannot accurately reflect the characteristics of the data and thus impair decisions related to

A. Elías is with Dep. of Applied Mathematics, Univ. of Malaga, Spain. E-mail: [aelias@uma.com](mailto:aelias@uma.com). S. Pineda is with the Dep. of Electrical Engineering, Univ. of Malaga, Spain. E-mail: [spinedamorente@gmail.com](mailto:spinedamorente@gmail.com). J. M. Morales is with the Dep. of Applied Mathematics, Univ. of Malaga, Spain. E-mail: [juan.morales@uma.es](mailto:juan.morales@uma.es).

This work was supported in part by the Spanish Ministry of Science and Innovation through project PID2020-115460GB-I00, and by the Andalusian Regional Government through project P20-00153. This project has also received funding from the European Social Fund and the European Research Council (ERC) under the European Union's Horizon 2020 research and innovation programme (grant agreement No 755705).

power system dispatch [4], [5], fault diagnosis [6], and state estimation [7]. Outlier detection can also help reveal consumer behavior, capture energy theft, find system vulnerabilities and failures, and improve service quality [4], [5], [8], [9], [10].

Surveys on outlier detection for smart grids and time series [3], [11], [12] have provided detailed taxonomies that classify the literature by groups of data analytic methodologies. Particularly, the authors [3] categorize outlier methods into SVM-based, proximity-based, and hybrid methods. More recently, [12] has provided an extensive taxonomy of the existing algorithms based on the different modules and parameters adopted, such as machine learning algorithms, feature extraction approaches, anomaly detection levels, computing platforms, and application scenarios. From the point of view of time series analysis, in [11] the authors propose differentiating between the type of input data (univariate or multivariate time series), outlier type (point, subsequence, or time series), and nature of the method (univariate or multivariate). Hence, this literature is rich in outlier detection methods but, unfortunately, little attention has been paid to Functional Data Analysis (FDA), an approach that excels in the crucial job of *interpreting* and linking the detected outliers to the physical phenomenon that produces them [12].

More precisely, FDA [13], [14] is a branch of Statistics, which has been especially designed for high dimensional data whereby each observation is a function observed over a continuum. One smart meter time series can be framed within this context by considering each daily record as a complete function. To date, the taxonomy of outliers in FDA has distinguished between *magnitude outliers* and *shape outliers* by way of the *functional boxplot* [15] and the *outliergram* [16], respectively. However, when each function is indexed in time, the outlying temporal evolution and outlying periodical variation patterns have been ignored so far, a current gap in the literature of smart meters [3], [17], which this paper aims to fill. Only [18] proposes a bootstrap model-based method that takes into account the time dependency of one sample of a functional time series to detect periods with an abnormal daily evolution. Nevertheless, our purpose is different as we work with multiple samples of daily curves at the same time, one for each meter, moving our problem to the realm of high dimensional functional time series [19], [20].

Hence, leveraging results from FDA, we provide an outlier detection toolbox that is based on *functional depth measures* [21], [22]. These are order statistics that quantify the relative position of a function with respect to the full sample. The toolbox exploits the group structure to isolate individual meters with *different attributes* to the majority of the group and includes the celebrated magnitude [15] and shape [16] outlier

detection methods. On top of that, as the key add-on, we propose to use functional depth measures to detect *evolution outliers* too. These correspond to meters with abnormal inter-day evolution patterns or, in other words, individuals that do not follow the expected daily evolution mined from the group. With our new proposal, the outlier detection toolbox includes methods to unmask *magnitude*, *shape* and *evolution* characteristics.

Therefore, the main contributions of this work are:

- The design of a statistical framework based on high dimensional functional time series to address the analysis of data from multiple smart meters.
- The proposal of a dependency outlier method to unmask meters with abnormal evolution patterns based on functional depth measures.
- The proposal of a depth-measure transformation to emphasize daily trends and seasons so these key features of the original smart meter time series are retained.
- The introduction of a depth-based outlier detection toolbox for smart meter data that covers magnitude, shape, and dependency outliers that are interpretable and linkable with the physical characteristics of the feature under analysis.

The rest of the paper is organized as follows. Section II introduces the required functional definitions and the outlier detection methods are presented in Section III. Specifically, Subsection III-A and Subsection III-B review the outlier detection methods for magnitude and shape outliers, respectively, and introduce how to use them in the context of grouped smart meter data. Our proposal for evolution outliers is introduced in Subsection III-C. Then, in Section IV, we illustrate the use of the toolbox with real case studies. Finally, Section V presents the conclusions and some further research lines.

## II. MATERIALS AND METHODS

### A. From one meter time series to functional data

Formally, let  $\{\Gamma(u), u \in [1, p \times T]\}$  be one meter's feature that is recorded at  $p \times T$  points during  $T$  days, presenting a daily seasonality of length  $p$ . Then we consider each complete day record as a discrete realization of a functional process,

$$y_t(x) = \{\Gamma(u), u = x + p(t-1)\}, \quad (1)$$

$$t \in 1, \dots, T, \quad 1 \leq x \leq p,$$

where  $t$  represents the index of days and  $x \in [1, p]$  is the functions' domain of definition. In the context of smart meters, the domain is a range covering the twenty four hours of a day, typically from midnight to midnight. Since the resulting daily curves are indexed in time by  $t = 1, \dots, T$ , the literature has termed them Functional Time Series (FTS) [23].

For example, the top-left panel of Figure 1 represents the minute photo-voltaic energy generation recorded in a single household for a complete year. Here  $u$  measures the minute grid of time observations,  $T$  is the number of days (365), and  $p$  the number of records by day ( $60 \times 24$ ). The bottom-left panel shows one isolated week taken at random and the vertical lines represent the division between days. Finally, the FTS composed of  $T$  daily curves is plotted in the right panel.

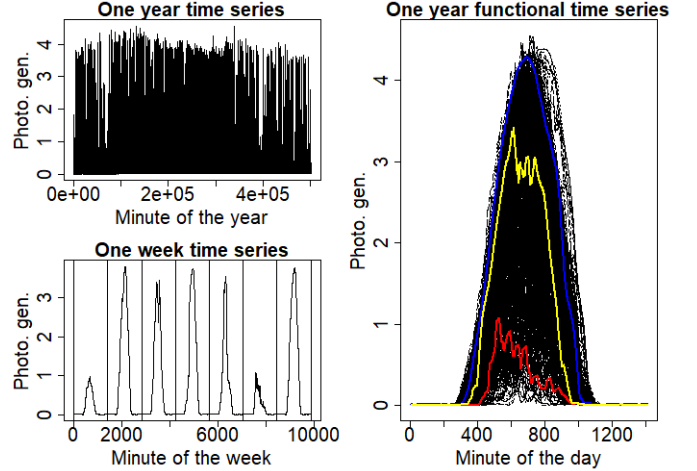


Fig. 1: From smart meters time series to functional time series.

### B. From discrete data to smooth functions and derivatives

Meters record data discretely and, therefore, we have discrete versions of the functions. For this reason, the first step in FDA is to represent each observation by the following linear expansion

$$y_t(x) \approx \sum_{k=1}^K c_k \phi_k(x),$$

being  $c_k$  constants and  $\phi_k(t)$  a set of given basis functions. The coefficients of the expansion  $c_k$  can be estimated by minimizing the least squares criterion and the set of basis functions must be selected by the user, being common choices the Fourier basis or polynomial splines [13], [14]. The step above is not only useful to get smooth functions and remove noise but to get derivative estimates. If the  $i$ -th derivative of the basis functions is defined, one can estimate the derivatives of the functions as follows

$$\partial_x^i y_t(x) \approx \sum_{k=1}^K c_k \partial_x^i \phi_k(x),$$

being  $\partial_x^i$  the  $i$ -th differential operator with respect to  $x$ . As we illustrate in the case studies, the first derivatives are powerful instruments to highlight shape characteristics of the curves.

### C. From multiple meters time series to functional data

Many meters provide many FTS, such as the one introduced in Equation (1). This data context can be framed into what is termed in the literature of FDA as a High Dimensional Functional Time Series [19], [20].

Let  $i = 1, \dots, N$  be the index of the meters. Then, a sample of high dimensional functions takes the following form:

$$\mathbf{y}(x) = \begin{bmatrix} y_1^1(x) & y_1^2(x) & \dots & y_1^N(x) \\ y_2^1(x) & y_2^2(x) & \dots & y_2^N(x) \\ \vdots & \vdots & \ddots & \vdots \\ y_T^1(x) & y_T^2(x) & \dots & y_T^N(x) \end{bmatrix}.$$

We denote by  $y^i(x)$  the  $i$ -th column of  $\mathbf{y}(x)$ . This is the FTS of one smart meter that is composed of  $y_1^i(x), \dots, y_T^i(x)$  daily

functions as in Equation (1). For instance, the right-hand panel of Figure 1 shows 365 days/functions for one household.

In contrast,  $y_t(x)$  is the  $t$ -th row corresponding to  $N$  functions for a given day  $t$ . This is a sample of  $N$  daily functions  $y_t^1(x), \dots, y_t^N(x)$  where each represents a meter.

In the following, to ease notation, we denote by  $y^1(x), \dots, y^N(x)$  the sample of  $N$  functions for a given day and  $y_1(x), \dots, y_T(x)$  the sample of  $T$  functions for a meter.

#### D. Functional depth measures

*Depth measures* are statistics that aim to provide an ordering of a set of data points when the sample space is not the real line [21]. Therefore, *functional depths* [22] provide an ordering of a sample of curves and, in consequence, related order statistics such as the median and quantiles. A particularly attractive property of functional depth measures for outlier detection purposes is that they are robust against outliers. In other words, their estimation is not biased or contaminated by the presence of outliers, making them useful even in those circumstances.

In general, there are two families of functional depths, namely, integrated and non-integrated ones [24]. The first class is defined by taking integrals over given collections of depths of low-dimensional projections of functions. In contrast, the non-integrated ones replace the integral by the infimum of these low-dimensional projections. Here, we opt for integrated functional depths because they are widely used in practice, are computationally efficient [25] and can deal with systematically missing parts, an important concern in data quality [3].

Formally, let  $FD$  be a general integrated functional depth. This statistic evaluates the centrality of a given function  $y(x)$  from a sample of functions  $y^1(x), \dots, y^N(x)$  with respect to its empirical distribution  $P_N$ . This empirical distribution belongs to a functional random variable taking values in a space of continuous functions defined in a domain  $[1, p]$ . For  $x \in [1, p]$ , we denote as  $P_{N,x}$  the marginal measure of  $P_N$  at slice  $x$  and its cumulative marginal distribution as  $F_{N,x}$ . Let  $\tilde{x} = 1, 2, \dots, p$ . Then, the empirical integrated functional depth is defined as

$$FD(y, P_N) = \sum_{\tilde{x}=1}^p w(\tilde{x}) \cdot D(y(\tilde{x}), P_{N,\tilde{x}}), \quad (2)$$

being  $w(\tilde{x})$  a weighting function that sums up to 1 and  $D$  a suitable univariate functional depth [24]. The weighting function allows focusing the analysis on different parts of the domain which, with smart meter data, corresponds to different periods of the day.

Equation (2) assigns a real number to each  $y(x)$ , typically between 0 and 1. The highest value is the deepest function, whereas lower values correspond to observations that are outsiders with respect to the sample of functions. Let us denote by  $y^{[1]}(x), \dots, y^{[N]}(x)$  the center-outward ordering being  $y^{[1]}(x)$  the deepest function and  $y^{[N]}(x)$  the most outlying curve of the sample. The statistic  $y^{[1]}(x)$  is a natural functional analog of the median and the literature has considered it as a robust estimator of the center of the distribution of the functions. As an illustration, the right-hand panel in Figure 1 shows, in yellow, the deepest function and in blue and red two of the

most outlying curves. Note how the most outlying curves are not simply the days with lower or higher values but the curves that remain in the most populated region just a short time.

Different  $D$  functions provide different integrated functional depths. For our purposes, we consider the well-known Modified Band Depth [26], which is defined by

$$MBD(y, P_N) = \frac{1}{p} \sum_{\tilde{x}=1}^p 2F_{N,\tilde{x}}(y(\tilde{x}))(1 - F_{N,\tilde{x}}(y(\tilde{x}))). \quad (3)$$

The  $MBD$  is built by plugging  $w(\tilde{x}) = 1/p$  and  $D(y(\tilde{x}), P_{N,\tilde{x}}) = 2F_{N,\tilde{x}}(y(\tilde{x}))(1 - F_{N,\tilde{x}}(y(\tilde{x})))$  in Equation (2). In plain words,  $MBD$  accounts for the average time that a given function lies inside all the possible bands built with pairs of the sample curves.

Finally, although it is not a functional depth, Equation (2) allows introducing the Modified Epigraph Index (MEI) [27], which is also used in outlier detection methods. It measures the mean proportion of curves lying above a given function  $y(x)$  and is defined as

$$MEI(y, P_N) = \frac{1}{p} \sum_{\tilde{x}=1}^p (1 - F_{N,\tilde{x}}(y(\tilde{x}))). \quad (4)$$

It is straightforward to see that  $MEI$  is obtained by replacing  $D(y(\tilde{x}), P_{N,\tilde{x}})$  by  $1 - F_{N,\tilde{x}}(y(\tilde{x}))$  and  $w(\tilde{x}) = 1/p$  in Equation (2).

### III. DEPTH-BASED OUTLIER DETECTION TOOLBOX

#### A. Magnitude outlier detection method

The functional boxplot was proposed by [15] and it is a particularly useful tool for determining magnitude outliers and visualizing the overall shape and dispersion of a set of functions. In essence, the authors extend the classical univariate Tukey's boxplot to the functional context. To do so, they propose functional analogs of the box and the whiskers, using the functional depth measures and related concepts we review here.

Let us focus for the moment on data of one single day  $t$ , denoted  $y^1(x), \dots, y^N(x)$ . Given this sample, we apply the  $MBD$  to obtain a ranking of functions  $y^{[1]}(x), \dots, y^{[N]}(x)$  that is used to build the functional boxplot.

Firstly, to find an analog of the classical box, the authors of [15] use the concept of central region (CR). This is defined as

$$\begin{aligned} CR_{.5} = & \{(x, y(x)) : \min_{r=1, \dots, \lceil \frac{N}{2} \rceil} y^{[r]}(x) \leq y(x) \\ & \leq \max_{r=1, \dots, \lceil \frac{N}{2} \rceil} y^{[r]}(x)\}, \end{aligned}$$

with  $\lceil \frac{N}{2} \rceil$  being the smallest integer greater than or equal to  $\frac{N}{2}$ . Intuitively, the  $CR_{.5}$  corresponds to the band that contains 50% of the deepest curves. Then, to define the functional whiskers, the upper and lower bounds of the  $CR_{.5}$  are inflated 1.5 times the functional inter-quantile range (IQR). In the functional context, IQR is defined as the difference between the upper and lower bounds of the CR. Finally, a function is determined as an outlier if it is outside the functional whisker at some time point of the domain.

The left-hand panel of Figure 2 presents an example of a functional boxplot. The data under analysis consist of 100 simulated curves with two magnitude outliers and two shape outliers. The central region is represented by the black band and its upper and lower whiskers are the two black lines attached to the central region by one vertical line at  $x = 0.5$ . Additionally, the functional median is included in yellow. Finally, there are two functions that are outside the whiskers at some point of the domain (red functions) and therefore, are potential magnitude outliers.

To this point, we have described the method for one single day data but, in our context, we have  $T$  days to be analyzed. To apply the ideas above in this case, we compute the functional boxplot for each day and account for the proportion of days that a given individual is outside the whiskers. Then, we highlight as an overall magnitude outlier those individuals that systematically outlie in a large proportion of days.

### B. Shape outlier detection method

Functions with abnormal shapes could still oscillate inside the whiskers of the functional Boxplot without being detected as an outlier (see the two blue lines of Figure 2). To overcome this drawback, the authors of [16] propose the outliergram, a visualization tool and algorithm that defines a rule to determine shape outliers even if they are hidden in the bulk of data.

As with the functional boxplot, we focus for a moment on data for one single day  $t$ . Once again, this is a sample of  $N$  daily functions  $y^1(x), \dots, y^N(x)$  where each function represents one meter.

Specifically, in [16] the authors study the mathematical relationship between MBD and MEI and prove that these statistics satisfy the following quadratic expression,

$$MBD(y, P_N) \leq a_0 + a_0 MEI(y, P_N) + a_1 n^2 MEI(y, P_N),$$

being  $a_0$  and  $a_1$  two parameters that are computed as  $a_0 = -2/N(N-1)$  and  $a_1 = 2(N+1)/(N-1)$ . Each function  $i$  has an associate pair  $(MBD(y^i, P_N), MEI(y^i, P_N)) \in \mathbb{R}^2$  and all the points must be below the parabola, the closer to the parabola, the more typical the shape. Additionally, as the authors show in extensive simulations, the closer to the parabola, the less the functions intersect and the more structured the data set is. Given this parabolic relationship, the authors propose to shift down this upper bound parabola by a given factor to define the rule to detect shape outliers.

The right-hand panel of Figure 2 presents an example of the outliergram. The theoretical parabola is in solid black and the shape outlier region is determined by the area below the dotted parabola. In the panel on the left, one can observe two curves (in blue) with an abnormal shape in comparison to the deepest curve (in yellow) and the central region. However, they are hidden inside the whiskers and not unmasked as a magnitude outlier by the functional boxplot. In contrast, the outliergram effectively detects the two curves as shape outliers, since the two corresponding points to these functions are below the dotted parabola. Finally, the two magnitude outliers (in red) are located in the points  $(0, 0)$  and  $(1, 0)$  of the outliergram, i.e. they have the minimum depth, equal to 0, and one is

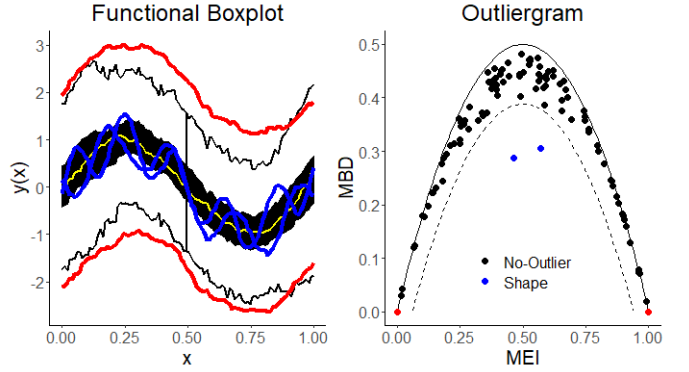


Fig. 2: Functional Boxplot (left panel) and Outliergram (right panel) for 100 simulated curves. Two magnitude and two shape outliers are included.

completely above, MEI equal to 0, and the other completely below the majority, MEI equal to 1.

As we do with the functional boxplot, we compute the outliergram for each day and account for the proportion of days that a given individual is below the lower parabola. Then, we highlight, as shape outliers, those individuals that systematically outlie in a large proportion of days  $T$ .

### C. Evolution outlier detection method

Our proposal aims to use functional depth measures to capture the dynamic daily evolution of smart meter data. With this goal, we use the FTS provided by each meter  $i$  i.e.  $T$  daily functions for each single meter, and we compute the depth values of each of the functions  $y_1(x), \dots, y_T(x)$  with respect the empirical distribution  $P_T$ . That is, for each  $t = 1, \dots, T$ , we obtain  $FD(y_t, P_T)$ . Hereafter, we denote  $FD(y_t, P_T)$ , as  $FD(t)$ , that is, the functional depth value of the day  $t$ . Our approach is focused on the analysis of these depths arranged as the following time series

$$\{FD(t), \quad t \in (1, \dots, T)\}.$$

To illustrate the intuition behind the proposal, see Figure 3. The top-left panel illustrates an FTS with a trend component. The deepest function is the green curve,  $t = 3$ , and the curves with the smallest depth values are the red and the black curves,  $t = 1$  and  $t = 5$ . The top-central panel arranges depth values as a time series  $FD(t)$  where each point is related to one curve. Then, the highest depth is observed at time point  $t = 3$  and the two lowest are observed at  $t = 1$  and  $t = 5$ . On the other hand, the bottom-left panel illustrates an FTS with a seasonal behavior, more particularly the magnitude of the curves is repeated each five functions and two seasons are included. Solid curves represent the first season and dotted lines the second season of the FTS. Now, the two green functions are the two deepest and correspond to curves  $t = 3$  and  $t = 8$ . The bottom-middle panel shows  $FD(t)$  where two peaks are presented corresponding to these two periods.

This toy example illustrates how depth measures are able to track the time position of each curve and how the corresponding time series of depths retain trend and seasonal features.

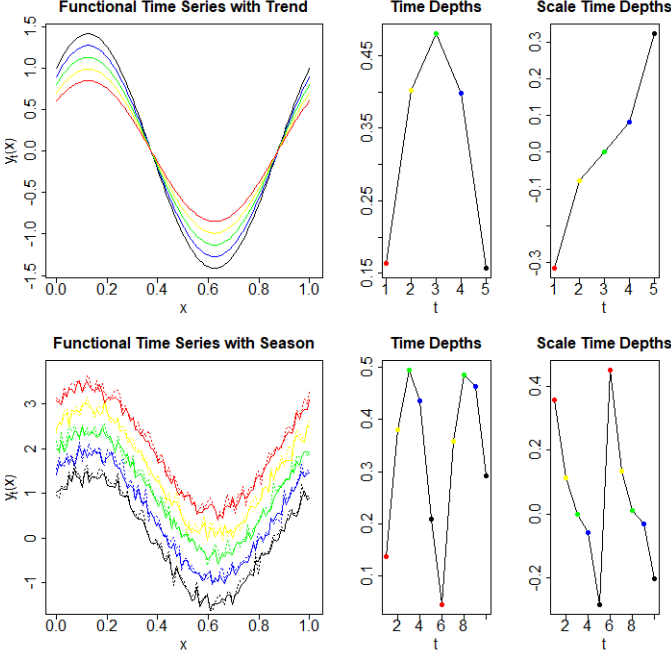


Fig. 3: Illustration of time series of depths,  $FD(t)$ , and time series of scaled depths,  $\widetilde{FD}(t)$  for two Functional Time Series.

However, depth measures only account for how far a function is from the center of symmetry and they do not discriminate between deviations above or below the central region. So, two functions with the same depth value might be in opposite locations with respect to the center. The example in the top panel of Figure 3 emphasizes this problem; curves in yellow and blue have a different overall position with respect to the center, one is above and the other below. Nevertheless, the depth values are not able to capture this feature.

To overcome this drawback, we propose an enrichment of the depth measures with the information provided by the Modified Epigraph Index (MEI) introduced in Equation (4). Using this concept, we introduce what we call the *scaled depth*, defined as

$$\widetilde{FD}(y, P_T) = sgn(MEI(y_{[1]}, P_T) - MEI(y, P_T)) \quad (5)$$

$$\times (FD(y_{[1]}, P_T) - FD(y, P_T)) \quad (6)$$

where  $sgn$  stands for the sign function and  $y_{[1]}$  is the functional median. The term (5) takes into account whether or not a function is above or below the median curve, being positive if it is above and negative otherwise. On the other hand, term (6) centers the FD in zero this value being associated with the deepest curve. Now, outlying functions below the median has a negative  $\widetilde{FD}$ , while this is positive for functions above the median.

Analogously to depth measures, the scaled depth measures provide a time series where each of the time points represents the value of a given day  $t$ ,

$$\{\widetilde{FD}(t), \quad t \in (1, \dots, T)\}$$

The time series of scaled depth is defined to capture the trend and seasonal patterns of the original time series. This is

illustrated in the right-hand panels of Figure 3 where the scaled depth measures are plotted. Now, the positive trend evolution is visually evident in the FTS with a trend (top panels) and with two seasons (bottom panels). Original smart meter time series with trends and seasons would also show trends and seasons in the scaled depth time series.

Given  $N$  meters, we thus have  $FD^i(t)$  and  $\widetilde{FD}^i(t)$  for  $i = 1, \dots, N$ . For simplicity, we continue the exposition for  $\widetilde{FD}^i(t)$  but everything can be extrapolated to  $FD^i(t)$ . The full set of individuals constitutes the following multivariate time series of scaled depths

$$\widetilde{\mathbf{FD}}(t) = [\widetilde{FD}^1(t), \widetilde{FD}^2(t), \dots, \widetilde{FD}^N(t)]$$

Daily dependent data must result in time series  $FD^i(t)$  and  $\widetilde{FD}^i(t)$  which variate in a structured way. Additionally, since we are focusing on meters that belong to a group, the multivariate time series must be synchronized sharing common movements between meters. Hence, deviations from this common evolution would determine an abnormal dependency pattern. To capture the overall time dependency pattern we compute the  $\alpha$ -trimmed mean of  $\widetilde{\mathbf{FD}}(t)$  [28] and we use it as a robust estimate of the overall evolution. This is

$$\mu\widetilde{\mathbf{FD}}(t) = \frac{1}{\lceil \alpha N \rceil} \sum_{r=1}^{\lceil \alpha N \rceil} \widetilde{FD}^{[r]}(t),$$

being  $\alpha \in [0, 1]$  and  $\widetilde{FD}^{[r]}(t)$  the  $r$ -order statistics. We consider as default  $\alpha = 0.5$ .

Then, we use the Euclidean distance between each  $\widetilde{\mathbf{FD}}(t)$  and the prototype  $\mu\widetilde{\mathbf{FD}}(t)$  to find individuals with a temporal evolution that is far from the prototype evolution, i.e.,

$$d(\widetilde{FD}^i(t), \mu\widetilde{\mathbf{FD}}(t)) = \sqrt{\sum_{t=1}^T (\widetilde{FD}^i(t) - \mu\widetilde{\mathbf{FD}}(t))^2},$$

Large values of  $d(\cdot, \mu\widetilde{\mathbf{FD}}(t))$  indicate that the dependency pattern is abnormal with respect to the prototype evolution.

The next step is to define a threshold or cutoff to objectively determine which is far enough away to be unmasked as an evolution outlier. For this purpose, we study the empirical distribution of the vector of distances  $\mathbf{d}$ . Intuitively, one might expect that it should be right-skewed given that we are dealing with squared values. However, to avoid distributional assumptions, we opt for a flexible adaptation by [29] of the classical Tukey's boxplot rule. Precisely, we highlight a given meter  $i$  as outlier if

$$d(\widetilde{FD}^i(t), \mu\widetilde{\mathbf{FD}}(t)) > Q_3(\mathbf{d}) + \gamma \times \exp^{3MC} \times IQR(\mathbf{d}),$$

where  $Q_3$  and  $IQR$  are the third quantile and the interquartile range,  $MC$  the medcouple statistics and  $\gamma$  a parameter to tune the length of the whiskers. The authors of [29] set it to 1.5 to leave roughly 1% of probability in both tails but, since we are only looking for right-tailed outliers, we consider  $\gamma = 0.72$  to leave approximately 5% only in the right tail of the distribution. Note that the flexibility of this rule comes from the fact that, if the distribution of  $\mathbf{d}$  is symmetric ( $MC = 0$ ), then the proposal by [29] turns out to be the classical Tukey's

TABLE I: Identifiers of the detected outliers by the toolbox.

	Zero derivative				First derivative				
	Meter id	M	S	E	$\tilde{E}$	M	S	E	$\tilde{E}$
Voltage	vol <sub>5746</sub>		✓		✓				
	vol <sub>6139</sub>	✓	✓		✓				
	vol <sub>7901</sub>	✓	✓	✓	✓				
	vol <sub>9019</sub>	✓							
	vol <sub>9922</sub>				✓				
	vol <sub>7951</sub>				✓				
Solar	sol <sub>9019</sub>				✓				
	sol <sub>6139</sub>					✓			
	sol <sub>3538</sub>						✓		

Boxplot. Therefore, it only corrects under departures from the symmetry assumption.

#### IV. NUMERICAL RESULTS

In this section we illustrate the outlier detection toolbox with real data. Concretely, we use the Pecan Street data set [1] that provides access to 1-minute records of smart meters from Austin over one year. We use voltage circuit data (25 households) and solar energy generation (19 households<sup>1</sup>) to illustrate the outlier detection toolbox.

In all the results, we have used the Modified Band Depth and the parameters are set with their default values as explained in Section III. To determine magnitude and shape outliers, an individual must be outlier more than 95% of the days considered in the data set. Additionally, for photo-voltaic data, we use the weighting function of Equation (2) proportional to the non-zero solar generation profiles obviating night time periods. For voltage data, we consider uniform weights. The toolbox is applied on the smooth level data and the first derivatives. To smooth the data and to estimate the derivatives, we use cubic B-splines and the number of basis functions  $K$  is selected to minimize the mean squared error [13], [14].

Table I shows the identifiers of the households that have been detected as magnitude outlier (M), shape outlier (S) or evolution outlier (E and  $\tilde{E}$  stand for time series of depths and time series of scaled depths, respectively). A household is considered as M or S if it is a magnitude or shape outlier in more than 95% of the days under analysis. Columns 2-5 include the outliers detected using the level data, while columns 6-9 report those found by using the first derivative. In what follows, we remark on the key learnings.

##### 1) Evolution outliers are not detected by other methods:

As Table I shows, the methodology proposed in this paper allows us to uncover outliers that are not caught by existing methods for detecting magnitude or shape functional outliers. In particular, although meter vol<sub>9019</sub> is not identified as a magnitude or shape outlier, this household follows an abnormal daily voltage evolution with respect to the group of households and therefore, it is classified as an evolution outlier. Subfigure 4a shows 305 daily curves for a non-outlier household (vol<sub>2818</sub>) and Subfigure 4b the corresponding daily

<sup>1</sup>Given the metadata of the Pecan Street data set, households 8565, 8386, 9922, 5746, 7951 and 7901 do not have photo-voltaic energy generation.

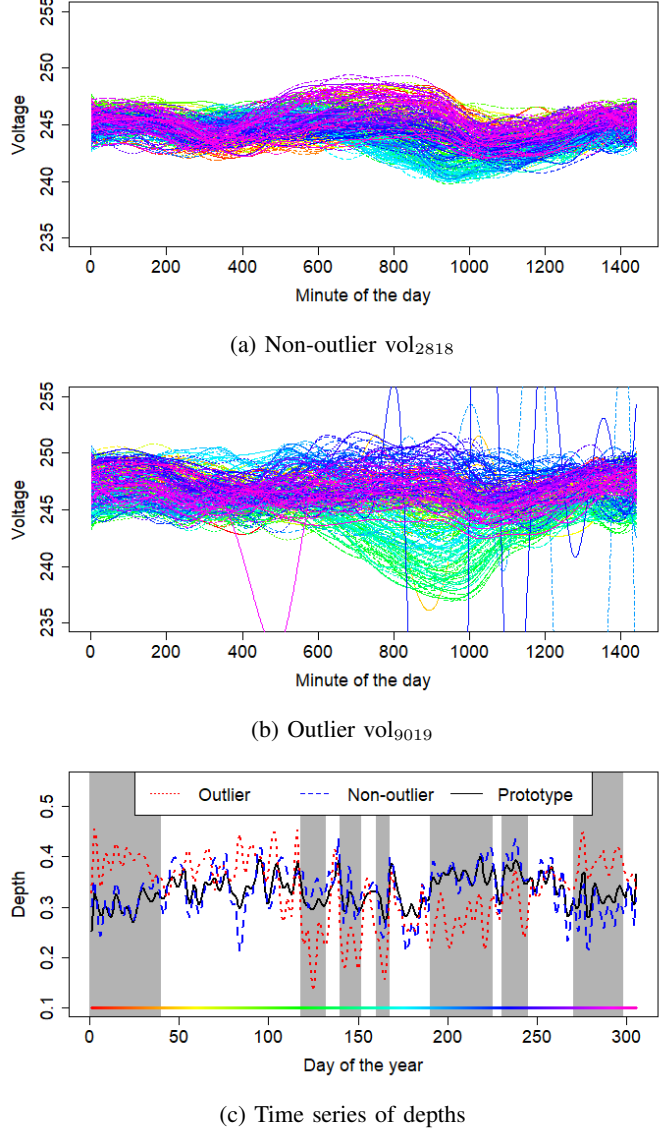
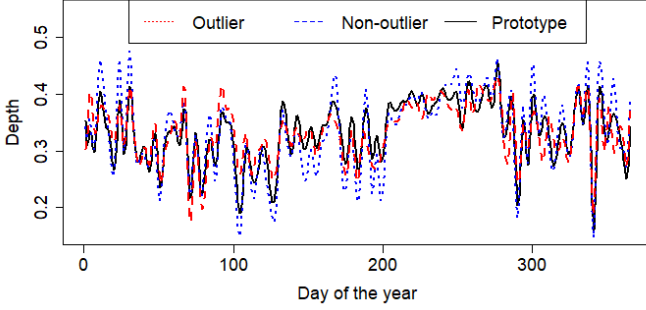


Fig. 4: Voltage circuit: evolution outlier not detected with other method.

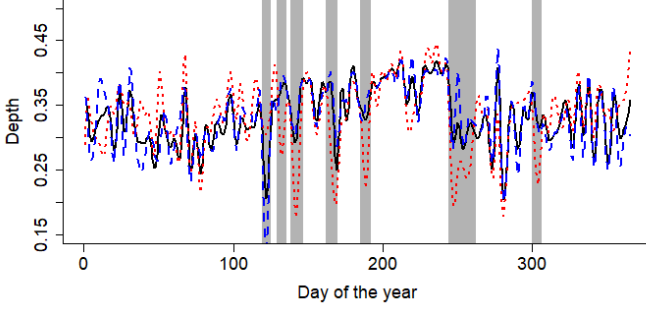
curves for the detected evolution outlier (vol<sub>9019</sub>). Each daily curve is colored with a rainbow palette associated with the calendar day, that is, similar colors are days which are close in time.

A preliminary visual inspection of Subfigure 4a and Subfigure 4b reveals the outlying nature of vol<sub>9019</sub> in comparison with vol<sub>2818</sub>. They show that voltage daily curves of the same period of time have a different relative magnitude position for the non-outlier and for the outlier. However, one should expect roughly synchronized evolution for two households fed by the same substation branch. Specifically, the outlier profile has a group of green curves located in low values of voltage, while they are located centrally for the non-outlier. Light blue curves are above the majority for the outlier household; and for the non-outlier, they are located below and in the middle of the majority of the curves.

The difference in the evolution is more evident in Subfig-



(a) Time series of depths computed on the zero derivative.



(b) Time series of depths computed on the first derivative.

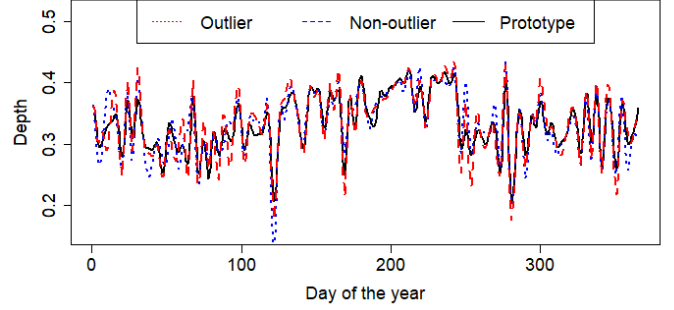
Fig. 5: Photo-voltaic energy generation: Computed depths on the derivatives allow detecting outliers not unmasked by the analysis without derivatives.

ure 4c where the time series of depths,  $FD(t)$ , are represented for the non-outlier and the outlier. Moreover, the prototype,  $\mu FD(t)$ , is plotted with a solid line. Here, the outlier (dotted line) moves far away from the prototype, while, in contrast, the non-outlier (dashed line) remains close to it.

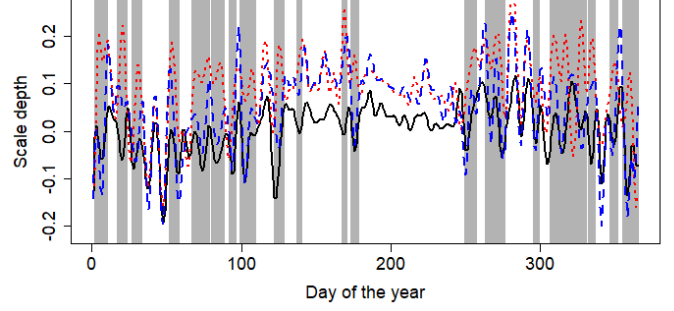
2) *First derivatives allow detecting those outliers not detected with level data:* Another remark from Table I is that the use of the first derivatives discloses those outliers not unmasked with the functions in levels. This is the case for the circuit voltage of the outlying households  $vol_{9922}$  and  $vol_{7951}$ , which are two of the just six households that do not have photo-voltaic energy generation. The effect of not having solar energy generation on the household circuit voltage is not large enough to be caught with level data, however, the derivatives intensify the shape differences and they are detected as magnitude outliers.

Similarly, the first derivatives allow highlighting households with abnormalities in terms of solar energy generation. Whereas magnitudes of solar profiles are determined by the amount of power generation installed, the shapes are highly influenced by the panels orientation and tilt. In fact, the two households  $sol_{6139}$  and  $sol_{9019}$ , which are detected as evolution outliers (E) in the first derivatives, have their solar panels set to the south, whereas the majority of the households are south-west-oriented<sup>2</sup>.

<sup>2</sup>Panel tilt is not available from the metadata of the Pecan Street data set to have the complete picture of the solar panel setting.



(a) Time series of depths.



(b) Time series of scaled depths.

Fig. 6: Photo-voltaic energy generation: Scaled depths detect outliers not detected by classical depths.

For a better understanding of these evolution outliers, Subfigure 5a shows the time series of depths of one outlier household ( $sol_{6139}$ ), one non-outlier household ( $sol_{4767}$ ) and the prototype. The time series of depths for the non-outlier and the outlier are not far from the prototype, meaning that their daily evolution is fairly similar. In contrast, if we consider the first derivatives, more discrepancies appear. To see this, Subfigure 5b represents the time depths of the same households and the prototype computed on the first derivatives where the outlier profile is farther from the prototype than the non-outlier (shaded grey regions).

This points to the fact that the analysis of the derivatives might capture the shape differences in the daily generation solar profile due to the differences of panel orientation and tilt. Therefore, our methodology can be useful, for example, to detect outliers in terms of panel settings when data of a group of meters with a similar panel configuration are available.

3) *Scaled depths unmask those outliers which are not detected with regular depths:* Time series of depths are not able to discern between positive and negative daily trends or peaks and valleys with seasonal data. This means that the time depth of a meter with a positive daily trend would behave similarly to the time depth of a meter with a daily negative trend. For example, a household with a systematic growth of voltage would provide time depths that are similar to a household whose voltage circuit systematically decreases. In contrast, scaled depths are especially defined to shed light on differences in these variations in trends and seasons. Table I

shows that the use of scaled depths ( $\tilde{E}$ ) with photo-voltaic solar energy generation captures the household  $\text{sol}_{3538}$  as outlier whereas it is not captured with other methods, including classical depths.

Figure 6 illustrates this particular case. More precisely, Subfigure 6a shows the regular time depths of the outlier household ( $\text{sol}_{3538}$ ) and one non-atypical ( $\text{sol}_{4767}$ ) computed on the first derivatives of solar energy generation. Both time series of depths are close to the prototype. However, the scaled depths  $\tilde{FD}$  represented in Subfigure 6b highlight periods where the atypical is remarkably far from the prototype (shaded grey regions).

Additionally, we see that the  $\tilde{FD}$  of the outlier is generally above the prototype when the differences with the prototype are large. This means that the solar setting of this household provides a daily profile with larger periods of growth (positive derivatives) than the majority of the households, especially at the start and end of the year. In fact, checking the Pecan Street metadata,  $\text{sol}_{3538}$  the third largest solar installation facing west and the smallest facing south. This setting produces a double-humped daily profile with a maximum peak of generation that occurs later in the day than that of the majority.

## V. CONCLUSION

This article has introduced an outlier detection toolbox supported by the theoretical framework of Functional Data Analysis. The underlying methodology takes advantage of the analysis of multiple grouped meters to extract joint information to overcome the lack of exogenous variables equally affecting all the meters.

To fill the absence of methodologies focused on temporal daily dependency, we propose an outlier detection method that is able to uncover evolution outliers that remain hidden with current methods. Furthermore, our outlier detection method proposal, in conjunction with the available methods from the literature, covers a wide and general class of possible atypical phenomena, namely, shape, magnitude, and evolution outliers. We believe that this classification might support practitioners in the crucial tasks of understanding the sources of the potential abnormality and supporting the decision to intervene.

Future lines of work are to explore the use of multivariate functional depth measures to incorporate functional covariates into the analysis, such as ambient temperature, module temperature and irradiation, and the upgrade of the outlier toolbox to deal with sets of very heterogeneous meters.

## REFERENCES

- [1] P. Street, "Real energy. real consumers. in real time," 2012. [Online]. Available: <http://www.pecanstreet.org/energy/>
- [2] A. Kanal, "Kaggle: Solar power generation data," 2020, <https://www.kaggle.com/anikannal/solar-power-generation-data/metadata>.
- [3] L. Sun, K. Zhou, X. Zhang, and S. Yang, "Outlier data treatment methods toward smart grid applications," *IEEE Access*, vol. 6, pp. 39 849–39 859, 2018.
- [4] E. W. S. Angelos, O. R. Saavedra, O. A. C. Cortés, and A. N. de Souza, "Detection and identification of abnormalities in customer consumptions in power distribution systems," *IEEE Transactions on Power Delivery*, vol. 26, no. 4, pp. 2436–2442, 2011.
- [5] S. Liu, Y. Liang, J. Wang, T. Jiang, W. Sun, and Y. Rui, "Identification of stealing electricity based on big data analysis," *Energy Reports*, vol. 6, pp. 731–738, 2020, 2020 The 7th International Conference on Power and Energy Systems Engineering.
- [6] W. Sun and J. Hou, "A mprm-based approach for fault diagnosis against outliers," *Neurocomputing*, vol. 190, pp. 147–154, 2016.
- [7] A. Jindal, A. Dua, K. Kaur, M. Singh, N. Kumar, and S. Mishra, "Decision tree and svm-based data analytics for theft detection in smart grid," *IEEE Transactions on Industrial Informatics*, vol. 12, no. 3, pp. 1005–1016, 2016.
- [8] D. Tanasa and B. Trouse, "Advanced data preprocessing for intersites web usage mining," *IEEE Intelligent Systems*, vol. 19, no. 2, pp. 59–65, 2004.
- [9] R. Vallakati, A. Mukherjee, and P. Ranganathan, "A density based clustering scheme for situational awareness in a smart-grid," in *2015 IEEE International Conference on Electro/Information Technology (EIT)*, 2015, pp. 346–350.
- [10] Z. Wang, G. Li, X. Wang, C. Chen, and H. Long, "Analysis of 10kv non-technical loss detection with data-driven approaches," in *2019 IEEE Innovative Smart Grid Technologies - Asia (ISGT Asia)*, 2019, pp. 4154–4158.
- [11] A. Blázquez-García, A. Conde, U. Mori, and J. A. Lozano, "A review on outlier/anomaly detection in time series data," *ACM Comput. Surv.*, vol. 54, no. 3, Apr. 2021.
- [12] Y. Himeur, K. Ghanem, A. Alsalemi, F. Bensaali, and A. Amira, "Artificial intelligence based anomaly detection of energy consumption in buildings: A review, current trends and new perspectives," *Applied Energy*, vol. 287, p. 116601, 2021.
- [13] J. Ramsay, J. Ramsay, B. Silverman, S. S. Media, and H. Silverman, *Functional Data Analysis*, ser. Springer Series in Statistics. Springer, 2005.
- [14] F. Ferraty and P. Vieu, *Nonparametric Functional Data Analysis: Theory and Practice*. Springer-Verlag New York, 2006.
- [15] Y. Sun and M. G. Genton, "Functional boxplots," *Journal of Computational and Graphical Statistics*, vol. 20, pp. 316–334, 2011.
- [16] A. Arribas-Gil and J. Romo, "Shape outlier detection and visualization for functional data: the outliergram," *Biostatistics*, vol. 15(4), pp. 603–619, 2014.
- [17] Y. Wang, Q. Chen, T. Hong, and C. Kang, "Review of smart meter data analytics: Applications, methodologies, and challenges," *IEEE Transactions on Smart Grid*, vol. 10, no. 3, pp. 3125–3148, 2019.
- [18] P. Raña, G. Aneiros, and J. M. Vilar, "Detection of outliers in functional time series," *Environmetrics*, vol. 26, no. 3, pp. 178–191, 2015.
- [19] Y. Gao, H. L. Shang, and Y. Yang, "High-dimensional functional time series forecasting," in *Functional Statistics and Related Fields*, G. Aneiros, E. G. Bongiorno, R. Cao, and P. Vieu, Eds. Cham: Springer International Publishing, 2017, pp. 131–136.
- [20] ———, "High-dimensional functional time series forecasting: An application to age-specific mortality rates," *Journal of Multivariate Analysis*, vol. 170, pp. 232–243, 2019, special Issue on Functional Data Analysis and Related Topics.
- [21] J. W. Tukey, "Mathematics and the picturing of data," in *Proceedings of the International Congress of Mathematics (Vancouver, 1974)*, vol. 2, 1975, pp. 523–531.
- [22] I. Gijbels and S. Nagy, "On a general definition of depth for functional data," *Statist. Sci.*, vol. 32, no. 4, pp. 630–639, 11 2017.
- [23] S. Hörmann and P. P. Kokoszka, *Functional Time Series*, ser. Handbook of Statistics. Netherlands: Elsevier B.V., 2012, vol. 30, pp. 157–186.
- [24] S. Nagy, I. Gijbels, M. Omelka, and D. Hlubinka, "Integrated depth for functional data: statistical properties and consistency," *ESAIM: Probability and Statistics*, vol. 20, 2016.
- [25] Y. Sun, M. G. Genton, and D. C. Nychka, "Exact fast computation of band depth for large functional datasets: How quickly can one million curves be ranked?" *Stat*, vol. 1, pp. 68–74, 2012.
- [26] S. López-Pintado and J. Romo, "On the concept of depth for functional data," *Journal of the American Statistical Association*, vol. 104, no. 486, pp. 718–734, Jun. 2009.
- [27] ———, "A half-region depth for functional data," *Computational Statistics & Data Analysis*, vol. 55, no. 4, pp. 1679–1695, Apr. 2011.
- [28] R. Fraiman and G. Muniz, "Trimmed means for functional data," *TEST*, vol. 10, no. 2, pp. 419–440, 2001.
- [29] M. Hubert and E. Vandervieren, "An adjusted boxplot for skewed distributions," *Computational Statistics & Data Analysis*, vol. 52, no. 12, pp. 5186–5201, 2008.